Bioorganic Chemistry 40 (2012) 39–47

Contents lists available at SciVerse ScienceDirect

Bioorganic Chemistry

journal homepage: www.elsevier.com/locate/bioorg

Role of histidine 225 in adenosylcobalamin-dependent ornithine 4,5-aminomutase

Caitlyn Makins [a], François N. Miros [a], Nigel S. Scrutton [b], Kirsten R. Wolthers [a,*]

[a] Department of Chemistry, University of British Columbia Okanagan, 3333 University Way, Kelowna BC, Canada V1V 1V7
[b] Manchester Interdisciplinary Biocentre, Faculty of Life Sciences, University of Manchester, 131 Princess Street, Manchester, M1 7DN, UK

ARTICLE INFO

Article history:
Received 13 July 2011
Available online 16 August 2011

Keywords:
Adenosylcobalamin
Pyridoxal 5′-phosphate
Radical isomerization
Ornithine 4,5-aminomutase

ABSTRACT

Pyridoxal 5′-phosphate (PLP), in the active site of ornithine 4,5-aminomutase (OAM), forms a Schiff base with N^{δ} of the D-ornithine side chain and facilitates interconversion of the amino acid to (2*R*, 4*S*) 2,4-diaminopentanoic acid *via* a radical-based mechanism. The crystal structure of OAM reveals that His225 is within hydrogen bond distance to the PLP phenolic oxygen, and may influence the pK_a of the Schiff base during radical rearrangement. To evaluate the role of His225 in radical stabilization and catalysis, the residue was substituted with a glutamine and alanine. The H225Q and H225A variants have a 3- and 10-fold reduction in catalytic turnover, respectively, and a decrease in catalytic efficiency (7-fold for both mutants). Diminished catalytic performance is not linked to an increase in radical-based side reactions leading to enzyme inactivation. pH-dependence studies show that k_{cat} increases with the ionization of a functional group, but it is not attributed to His225. Binding of 2,4-diaminobutyric acid to native OAM leads to formation of an overstabilized 2,4-diaminobutyryl–PLP derived radical. In the H225A and the H225Q mutants, the radical forms and then decays, as evidenced by accumulation of cob(III)alamin. From these data, we propose that His225 enhances radical stability by acting as a hydrogen bond acceptor to the phenolic oxygen, which favors the deprotonated state of the imino nitrogen and leads to greater resonance stabilization of the 2,4-diaminobutyryl–PLP radical intermediate. The potential role of His225 in lowering the activation energy barrier to mediate PLP-dependent radical rearrangement is discussed.

1. Introduction

The fermentation of ornithine *via* the Stickland reaction has been extensively studied in the anaerobic bacterium *Clostridia sticklandii,* first isolated from San Francisco black mud in 1954 [1,2]. Recent genome sequencing and annotation has revealed that this metabolic pathway – an important source of energy and carbon – extends to a number of bacterial species in the Firmicute phylum, including the pathogenic microbe *Clostridia difficile* [3–5]. Ornithine 4,5-aminomutase (OAM)[1] catalyzes the second step in the oxidative breakdown of the amino acid, converting D-ornithine to 2,4-diaminopentanoic acid (DAP). In the third step, DAP dehydrogenase catalyzes the NAD^+-dependent oxidation of DAP to form 2-amino 4-ketopentoate, which is then further catabolized to acetate and alanine [4].

The 1,2-amino shift performed by OAM is considered energetically challenging as it involves breakage of chemically inert C–H and C–N bonds. OAM overcomes this thermodynamic barrier with radical-based catalysis that is initiated and propagated by the enzyme's adenosylcobalamin (AdoCbl) and pyridoxal 5′-phosphate (PLP) cofactors. The unusual rearrangement reaction is proposed to occur via the following mechanism. In the precatalytic state, PLP is covalently bound via a Schiff base (imine) to Lys629 [6]. D-ornithine displaces Lys629, forming an imine link (external aldimine) through the N^{δ} atom of the side chain (Fig. 1). Following transaldimination, the Co–C bond of AdoCbl undergoes homolytic rupture, generating a highly reactive carbon-centered 5′-deoxyadenosyl radical and cob(II)alamin. The 5′-deoxyadenosyl radical abstracts the C4 hydrogen atom from the D-ornithinyl–PLP aldimine producing a substrate radical **1**, which undergoes internal addition to the imine N to form an aziridylcarbinyl–PLP radical adduct **2** [7]. Ring opening leads to formation of a product-like

Abbreviations: AdoCbl, adenosylcobalamin; OAM, ornithine 4,5-aminomutase; 5,6-LAM, lysine 5,6-aminomutase; PLP, pyridoxal 5′-phosphate; TIM, triosephosphate isomerase; DABA, 2,4-diaminobutyric acid; DAP, 2,4-diaminopentanoic acid; DAPDH, 2,4-diaminopentanoic acid dehydrogenase; AEBSF, 4-(2-aminoethyl) benzenesulfonyl fluoride hydrochloride; SDS-PAGE, sodium dodecyl sulfate polyacrylamide gel electrophoresis; HEPES, *N*-(2-hydroxyethyl)piperazine-N′-2-ethanesulfonic acid; NAD^+, *β*-nicotinamide adenine dinucleotide; MES, 2-morpholinoethanesulfonic acid monohydrate; EPPS, 4-(2-hydroxyethyl)piperazine-1-propanesulfonic acid; TRIS, tris(hydroxymethyl)aminomethane; CHES, 2-(cyclohexylamino)-1-ethanesulfonic acid; NTA, nitrilotriacetic acid.

* Corresponding author. Fax: +1 250 807 8009.
E-mail address: kirsten.wolthers@ubc.ca (K.R. Wolthers).

0045-2068/$ - see front matter © 2011 Elsevier Inc. All rights reserved.
doi:10.1016/j.bioorg.2011.08.003

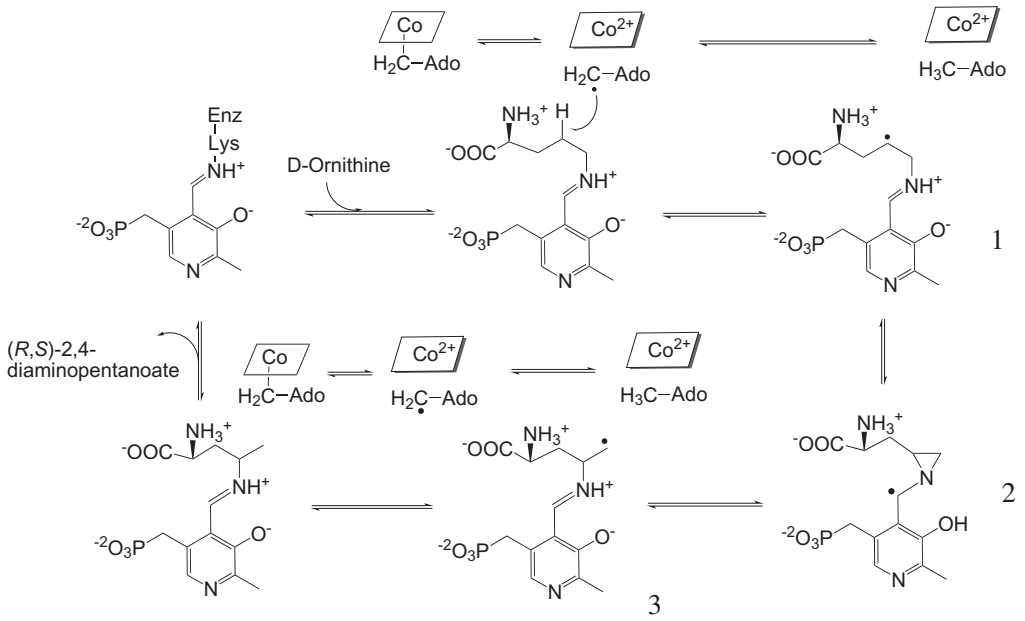

Fig. 1. A proposed catalytic mechanism for the reaction of OAM. In the resting state of the enzyme, PLP is covalently bound to Lys629. D-ornithine displaces the internal aldimine linkage and forms an imine bond through the N^{δ} atom of the side chain (the migrating amine). Formation of the external aldimine induces homolysis of the AdoCbl Co–C bond generating the low spin cob(II)alamin intermediate and the highly reactive 5′-deoxyadenosyl radical. The latter carbon-centered radical then abstracts a hydrogen atom from the C4 atom of the ornithyl side chain forming 5′-deoxyadenosine and the substrate-like radical, **1**. Internal addition of **1** forms an aziridylcarbinyl–PLP radical, **2**, which opens via homolytic fission to generate the product-like radical, **3**. The catalytic cycle is complete with abstraction of the hydrogen atom by **3** from 5′-deoxyadenosine, release of the 2,4-diaminopentanoate product and recombination between the 5′-deoxyadenosyl radical and cob(II)alamin.

radical intermediate **3**, which reabstracts a hydrogen atom from 5′-deoxyadenosine. AdoCbl is reformed with geminate recombination between the 5′-deoxyadenosyl radical and cob(II)alamin. Release of product from PLP completes the catalytic cycle.

OAM is an $\alpha_2\beta_2$ heterodimer comprising two strongly associated subunits, OraS (12.8 kDa) and OraE (82.9 kDa) [6]. The crystal structures of OAM [8] and that of structurally related lysine 5,6-aminomutase [9] reveal that radical propagation from AdoCbl to the PLP-bound substrate requires large-scale protein conformational motion. In the substrate-free form of OAM, the Rossmann-like domain, which harbors the AdoCbl cofactor, is tilted away from the triosephosphate isomerase (TIM) barrel, the site of PLP binding [8]. In this "open" conformation, the 5′-deoxyadenosyl moiety of AdoCbl is exposed to the solvent and is ~23 Å away from the PLP and substrate binding site. Lys629 originates from the Rossmann domain. Thus, in the absence of substrate, the Lys629-PLP internal aldimine locks the enzyme in this "open" conformation, excluding AdoCbl from the active site. Substrate binding releases the internal aldimine link, allowing rotation of the Rossmann domain and positioning of the 5′-deoxyadenosyl moiety next to the PLP-bound substrate for radical propagation.

OAM turnover with D-ornithine does not result in a steady state accumulation of cob(II)alamin that is detectable by UV-visible or by electron paramagnetic resonance (EPR) spectroscopy. This suggests that radical chemistry mediated by PLP is fast compared to more rate-limiting steps in the catalytic cycle such as transaldimination or large-scale protein conformational changes. In contrast, binding of the substrate analogue 2,4-diaminobutyric acid (DABA) to OAM leads to the formation of an overstabilized PLP-organic radical. It is believed that formation of the 2,4-diaminobutyryl–PLP external aldimine leads to abstraction of the C4 hydrogen from the amino acid side chain by the 5′-deoxyadenosyl radical. The resulting unpaired electron on C4 is proximal to the Schiff base and is stabilized by delocalization through the conjugated π orbital system of the pyridine ring and imine moiety [10]. The EPR spectrum of the OAM–DABA complex shows that the 2,4-diaminobutyryl–PLP radical species is strongly spin coupled to the low spin Co^{2+} of cob(II)alamin, indicating that the two unpaired electrons are separated by a distance of <6 Å [11]. The EPR data demonstrate that OAM adopts a catalytically active "closed" state that positions AdoCbl within the active site, similar to that observed in the structures of related AdoCbl-dependent mutases and eliminases [12,13].

In addition to serving as a structural anchor, *ab initio* molecular orbital calculations indicate that PLP also facilitates radical chemistry by introducing unsaturation into the migrating N^{δ} of the substrate (thereby lowering the energy barrier for intramolecular isomerization; steps 3–6 in Fig. 1) and controlling the stability of radical intermediates through captodative effects [14]. The X-ray crystal structure of OAM extends the profile for enzymatic control of radical catalysis beyond that of the PLP cofactor [8], revealing residues directly coordinated to the cofactor and their potential role in facilitating radical rearrangement of the PLP-bound substrate (Fig. 2). Of particular interest is His225, which forms a hydrogen bond to the PLP phenolic oxygen. Given that the imidazole side chain can act both as a hydrogen bond donor or acceptor to the phenolic oxygen, the active site residue can potentially influence the pK_a of the Schiff base of the PLP external aldimine. Thus, the location of His225 suggests a possible role in catalysis and/or radical stabilization by direct participation in proton transfer to the PLP aldimine in one or more steps in the catalytic mechanism.

Previous studies of PLP-dependent enzymes, which catalyze the more classical polar reactions described for the cofactor, have noted the importance of the protonation state of the Schiff base in catalysis and stabilization of catalytic intermediates, but little is known how critical tautomerization is in catalysis of PLP-dependent radical enzymes [15]. The goal of this study was to investigate the role of His225 in mediating PLP-radical chemistry in OAM through its interaction with the PLP phenolic oxygen. H225A and H225Q variants of OAM were created, and both catalytic activities and abilities to stabilize PLP-radical intermediates were studied through UV-visible spectroscopy. To facilitate theses studies, we cloned and purified a recombinant form of DAP dehydrogenase

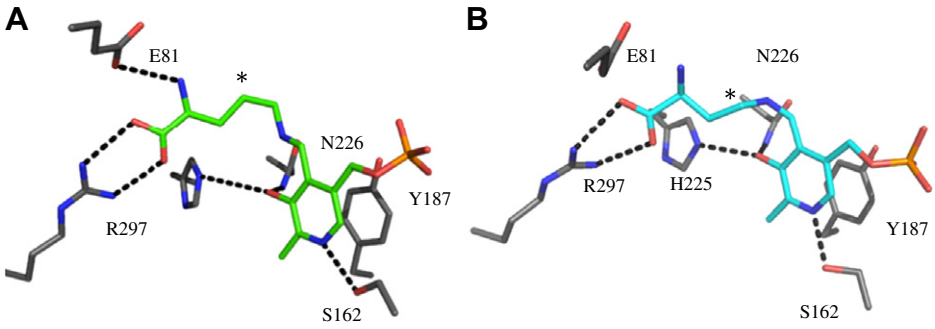

Fig. 2. A covalent imine link forms between D-ornithine (panel A) and 2,4 -diaminobutyric acid (panel B) in the PLP active site of anaerobically soaked OAM crystals. His225 and Asn226 are shown to hydrogen bond (black dashed line) to the phenolic group of PLP. The α-carboxylate of D-ornithyl–PLP (green sticks) and 2,4-diaminobutyryl–PLP (cyan sticks) are stabilized through a salt bridge with the guanidinium side chain of Arg297. Selected residues of the active site are shown as atom colored sticks with grey carbons (black dotted line). The carbon atom targeted for hydrogen atom abstraction by the 5′-deoxyadenosyl radical in marked by a star. PDB ID: 3KOZ (A) and 3KOX (B). (For interpretation of the references to colour in this figure legend, the reader is referred to the web version of this article.)

from *C. difficile* and used the enzyme to measure the turnover of OAM by a coupled assay. We also performed dead-end inhibition studies with 2,4-diaminobutyric acid to determine if the mutations affect the binding affinity of the inhibitor. Our results show that mutation of His225 attenuates PLP-mediated radical rearrangement. While His225 does not appear to affect the trajectories of radical intermediates during D-ornithine turnover, it does contribute to the overstabilization of the 2,4-diaminobutyryl–PLP radical, and the mechanism for radical stabilization is discussed.

2. Materials and methods

2.1. Materials

AdoCbl, PLP, D-ornithine, DL-2,4-diaminobutyric acid, and protease inhibitors (AEBSF, aprotinin, benzamidine) were obtained from Sigma. The Ni^{2+}-nitrilotriacetic acid (Ni–NTA) column and Q-sepharose High Performance resins were from GE Biosciences. Restriction endonucleases were from New England Biolabs, and *Pfu* Turbo DNA polymerase (Agilent Technologies) and Rosetta (DE3)pLysS competent cells were purchased from EMD Biosciences.

2.2. Cloning and expression of (2R,4S)-2,4-diaminopentanoate dehydrogenase (DAPDH)

The coding sequence for DAPDH was amplified from *C. difficile* genomic DNA (obtained as a gift from the Sanger Institute) with *Pfu* Turbo DNA polymerase using the primers 5′-CAT AAG TAG **CAT ATG** AGA AAA GTA AGA GTA GGA ATA TGG-3′ (forward primer) and 5′-TGA TAC GAT **AAG CTT** ATT AGC CTT TGA TTC TTC TTC C 3′ (reverse primer), which contain the NdeI and HindIII restriction sites (shown in boldface type), respectively. The PCR cycle parameters were as follows: 94 °C for 4 min followed by 30 cycles of 94 °C for 45 s, 53 °C for 1 min, and 72 °C for 6 min followed by a final 10 min extension at 72 °C. The PCR product was digested with NdeI and HindIII and inserted into the pET41a vector (EMD Biosciences), which had been digested with the same restriction enzymes. The ligation mixture was transformed into *Escherichia coli* strain XL1 Blue (Agilent). The cloning strategy inserted a hexahistidine tag onto the C-terminus of DAPDH and the resulting plasmid was designated pET-DAPDH. Sequencing of the plasmid by the DNA Sequencing Laboratory at University of British Columbia, Vancouver, Canada confirmed that no PCR-induced errors had occurred. pET-DAPDH was transformed into *Escherichia coli* strain Rosetta(DE3)pLysS, and a single transformed colony was used to inoculate LB medium (5 ml) containing ampicillin (100 μg/ml) and chloramphenicol (35 μg/ml), and the culture was grown for 8 h at 37 °C. The 5 ml culture was used to inoculate LB medium (200 ml) with ampicillin (100 μg/ml) and chloramphenicol (35 μg/ml), which was subsequently grown at 37 °C for 16 h. Ten milliliters from the 200 ml starter culture was used to inoculate Terrific Broth (0.5 l) containing ampicillin (100 μg/ml). The culture was grown at 32 °C with shaking (220 rpm) until the culture reached an optical density at 600 nm of 1.0, at which time isopropyl β-D-1-thiogalactopyranoside (0.1 mM) was added. The temperature of the incubator was reduced to 25 °C, and the culture was allowed to grow for a further 16 h. Cells were harvested by centrifugation (4000 g, 15 min, 4 °C), and the cell pellet was stored at –20 °C until purification.

2.3. Construction of OAM mutants

The H225A and H225Q mutations were introduced into the pOAMH2 vector [11] harboring the C-terminal hexahistidine tagged OAM from *C. sticklandii* OAM, using the QuikChange site directed mutagenesis kit (Stratagene, La Jolla). The complementary primers for the H225A mutants are 5′-CAG ATA GAT GGA GCG GCT AAT GCA AAC GCT ACA G-3′ and 5′-CTG TAG CGT TTG CAT TAC GCG CTC CAT CTA TCT G-3′. The sense and antisense oligonucleotides for the H225Q mutant are 5′-CAG ATA GAT GGA GCG CAG AAT GCA AAC GCT ACA G-3′ and 5′-CTG TAG CGT TTG CAT TCT GCG CTC CAT CTA TCT G-3′, respectively. The primers were obtained from MWG (Covent Garden, England). The sequence of the H225A and H225Q mutations was confirmed with DNA sequencing by MWG (Covent Garden, England).

2.4. Enzyme preparation

Purification of OAM and the H225A and H225Q mutants was performed as previously described [11]. DAPDH was purified in one chromatographic step using the following protocol. Rosetta(-DE3)pLysS cells (20 g, wet weight) overexpressing DAPDH were resuspended in 50 mL of 50 mM Tris-HCl, pH 7.5, containing AEBSF (0.2 mM), aprotinin (10 μg/mL) and benzamidine (2 mM). Cells were disrupted by sonication (5 s pulses separated by a 50 s interval for 15 min, power setting 22%) using a Misonix sonicator. The cell suspension was clarified by centrifugation at 25,000 g for 45 min. Imidazole (20 mM) and NaCl (0.5 M) were added to the supernatant, which was then applied to a 5 ml Ni^{2+}-nitrilotriacetic acid column equilibrated with 50 mM Tris-HCl, pH 7.5, 0.5 M NaCl, and 20 mM imidazole. The column was washed with 30 mL of 50 mM Tris-HCl, 0.5 M NaCl, pH 7.5 and 20 mM imidazole, and then 25 mL of 50 mM Tris-HCl, 0.5 M NaCl, pH 7.5 with 40 mM imidazole. The protein was eluted with a linear gradient to 500 mM imidazole. Fractions containing DAPDH were pooled and

dialyzed against 50 mM Tris-HCl, pH 7.5, 1 mM EDTA and 5 mM 2-mercaptoethanol for 16 h at 4 °C. The dialysate was concentrated using Centricons with a 30 kDa MW cutoff filter, flash-frozen in liquid nitrogen after making 20% glycerol stocks, and stored at –80 °C. Protein concentrations were determined by the Lowry method using bovine serum albumin as a standard.

2.5. Coupled enzyme assays

OAM activity was measured using a coupled spectrophotometric assay with DAPDH. Kinetic assays were performed in a 1.0 mL volume at 25 °C using a 1 cm path length cuvette. OAM activity was measured by recording the absorbance change at 340 nm associated with the reduction of NAD^+ ($\Delta\varepsilon = 6220\ M^{-1}\ cm^{-1}$). Purified recombinant OAM is devoid of cofactor; therefore, to make a functionally active holoenzyme, equimolar amounts of PLP and AdoCbl were added to the apo-form of the protein. The reaction mixtures contained 50 mM NH_4^+EPPS, pH 8.5, 100 nM holoOAM, 100 nM DAPDH, 0.5 mM NAD^+ and variable concentrations of D-ornithine (47–2265 μM). For inhibition assays, the reaction mixtures contained the same components except for the addition of variable concentrations of 2,4-diaminobutyric acid. Reactions were performed under dim light and were initiated with the addition of D-ornithine. Data from the substrate concentration dependence experiments were fit to the Michaelis–Menten equation, while data for the inhibition studies were fit with nonlinear least-squares analysis to the equation for competitive inhibition (Eq. (1)) using the computer program Origin, version 8.5 (MicroCal Software Inc.).

$$v_i = \frac{VA}{K_m(1 + I/K_i) + A} \quad (1)$$

where v_i is the initial velocity, V is the maximal velocity, A is the concentration of D-ornithine, K_m is the Michaelis constant for D-ornithine, I is the inhibitor concentration and K_i is the inhibition constant. The pH dependence assays of maximal activity were measured in a triple-component buffer (25 mM CHES, 25 mM HEPES and 25 mM MES) in a 1 mL reaction containing 100 nM holo-OAM, 100 nM DAPDH, 0.5 mM NAD^+ and 2.5 mM D-ornithine. The pH titration data were fit to the following equation (Eq. (2)), where the protonation of an ionizable group leads to an increase in activity.

$$Y = \frac{Y_{max} - Y_{min}}{1 + 10^{pK-pH} + Y_{min}} \quad (2)$$

where Y is the observed turnover rate and Y_{max} and Y_{min} are the maximal and minimal turnover rates at high and low pH, respectively.

2.6. Anaerobic UV-visible spectroscopy

Anaerobic UV-visible spectroscopic assays were performed in a Belle Technology glove box (O_2 < 5 ppm) using a Hitachi U-1800 spectrophotometer at 25 °C. Buffer (100 mM NH_4^+EPPS, pH 8.5) was purged for 2 h with nitrogen and then brought into the glove box and allowed to equilibrate for 18 h in an oxygen-free environment. Solid AdoCbl, PLP, D-ornithine, and DL-2,4-diaminobutyric acid were introduced to the glove box and dissolved in anaerobic buffer. A concentrated protein sample (2 ml of 12 mg/ml) was introduced into the glove box and gel-filtered using a 10 ml Econo-pack column (Bio-Rad) equilibrated with anaerobic buffer. A reference spectrum was recorded using buffer alone. For reactions involving the holoenzyme, a 1 ml reaction mixture contained 15 μM apo-OAM, 15 μM PLP, and 15 μM AdoCbl in 100 mM NH_4^+EPPS, pH 8.5. The reaction was initiated by the addition of 2.5 mM D-ornithine or 2.5 mM DABA, and spectra were recorded from 700 to 300 nm every 60 s for 20 min.

2.7. Aerobic UV-visible spectroscopy

Aerobic UV-visible spectral assays were performed on a Perkin Elmer Lambda 25 spectrophotometer at 25 °C. The 1 ml reaction contained 15 μM apo-OAM, 15 μM PLP, and 15 μM AdoCbl in 100 mM NH_4^+EPPS, pH 8.5. The reaction was initiated with the addition of 2.5 mM D-ornithine or 2.5 mM DL-2,4-diaminobutryic acid, and the spectra were recorded from 700 to 300 nm every minute for 20 min. UV-visible spectral studies with the PLP-bound form of the enzyme contained 15 μM apo-OAM and 15 μM PLP in 100 mM NH_4^+EPPS, pH 8.5 in 1 mL. The spectra of PLP-bound OAM was recorded from 700 to 300 nm before and 5 min after the addition of 2.5 mM D-ornithine or DL-2,4-diaminobutyric acid.

3. Results

3.1. Purification of DAPDH

The genes associated with anaerobic oxidative degradation of L-ornithine are found within a gene cluster conserved across several species of *Clostridiaceae*, including the pathogen *C. difficile* [4]. The gene for DAPDH, located at the 5' end of the gene cluster, was cloned from *C. difficile* genomic DNA in order to measure steady state turnover of OAM via a coupled UV-visible spectrophotometric assay. The high level of DAPDH amino acid sequence similarity (84%) between the two *Clostridia* species, suggests that the enzyme from *C. difficile* can substitute for the *C. sticklandii* counterpart in measuring OAM turnover. Following heterologous bacterial expression, the C-terminally hexahistidine tagged DAPDH was purified to homogeneity in one column purification step using Ni–NTA affinity resin (Fig. S1). The apparent molecular weight of the enzyme (41 kDa) determined from SDS-PAGE closely matches the predicted molecular weight of 40,551 Da for a DAPDH hexahistidine tagged protein. Given that DAPDH from *C. sticklandii* has a 1000-fold higher specificity for NAD^+ compared to $NADP^+$ [4,16], the former oxidized coenzyme was used in the steady state kinetic assays described below.

3.2. Steady state coupled assays

The steady state kinetic parameters for wild type OAM and the H225A and H225Q mutants were determined using a coupled assay (described in Materials and methods), where enzyme activity was measured by following an absorbance increase at 340 nm, corresponding to reduction of NAD^+ to NADH. The turnover number for wild-type OAM was 2.9 ± 0.1 s^{-1}, similar to that previously reported [17]. Substitution of His225 with glutamine resulted in a 3-fold reduction in k_{cat} (Table 1). Removal of the imidazole moiety and disruption of hydrogen bonding to the phenolic group of PLP achieved in the H225A mutant had a more substantial effect on the turnover rate, decreasing it 10-fold. The K_m for D-ornithine is 190 ± 13 μM for wild type OAM and 453 ± 34 μM and 140 ± 5 μM for the H225Q and H225A mutants, respectively. Consequently, the enzyme specificity (k_{cat}/K_m) decreases by the same magnitude (7-fold) in both the mutants ($2.2 \times 10^3\ M^{-1}\ s^{-1}$) compared to the native enzyme ($15.2 \times 10^3\ M^{-1}\ s^{-1}$). The inhibition constant, K_i, for DABA also increased the same magnitude in both the H225A (95 ± 25 μM) and H225Q (98 ± 17 μM) mutants compared to wild type (5 ± 1 μM), indicating that His225 contributes to inhibitor binding.

3.3. pH dependence on k_{cat}

Given that the steady state kinetic assays were performed at pH 8.5, it is likely that the imidazole ring of His225 is neutral. In this ionization state, the residue may be acting as a general base to

Table 1
Summary of steady state kinetic parameters for wild type and the H225A and H225Q mutants of OAM.

Enzyme	k_{cat} (s^{-1})	K_m (D-orn) μM	K_i (DABA) μM	k_{cat}/K_m (D-orn) × 10^3 M^{-1} s^{-1}
Wild type	2.9 ± 0.1	190 ± 13	4.6 ± 0.6	15.2 ± 1.2
H225Q	1.0 ± 0.1	453 ± 34	98 ± 17	2.2 ± 0.2
H225A	0.3 ± 0.1	140 ± 5	95 ± 25	2.2 ± 0.1

the phenolic group, increasing the pK_a of the imino nitrogen. As His225 was shown to affect OAM turnover, the pH dependence of k_{cat} was measured to determine if the protonation state of the imidazole base influences steady state kinetic parameters. For wild type OAM and the His225 mutants, k_{cat} increased at higher pH and plots of log k_{cat} versus pH (Fig. 3) had a limiting slope of 1 on the acidic limb, indicating that for each variant of OAM, one ionizable group limits turnover. A fit of Eq. (2) to the data produced pK_a values of 7.1 ± 0.1, 7.6 ± 0.1, and 7.4 ± 0.2 for wild type, H225A and H225Q mutants, respectively. The protonation state of His225 does not limit steady state catalysis, as the pH profiles and calculated pK_a values are similar between the three forms of OAM.

3.4. Anaerobic UV-visible spectroscopic assays

The binding of D-ornithine to holo-OAM induces UV-visible absorbance changes, most notably a decrease in absorbance at 416 nm caused by the formation of the external aldimine and a small reduction in absorbance at 525 nm demonstrating homolysis of AdoCbl (Fig. S2). Unlike the mutase family of AdoCbl-dependent enzymes, the cob(II)alamin species (indicated by an absorbance peak at 470 nm) does not accumulate to steady state levels that are observable by UV-visible spectroscopy or EPR [11]. However, prolonged turnover with D-ornithine, even in the absence of O_2, does lead to conversion of the undetectable cob(II)alamin intermediate to cob(III)alamin, and this is spectrally evident by an absorbance increase at 358 nm. Cob(III)alamin leads to enzyme inactivation, as this oxidative state of the cofactor cannot recombine with the 5′-deoxyadenosyl radical to regenerate AdoCbl for the next round of catalysis. The rate constant for cob(III)alamin formation is 0.08 min^{-1}. Spectral perturbations upon the addition of D-ornithine to H225Q or H225A are similar to that of wild type as all three show a decrease at 410 nm indicating binding of

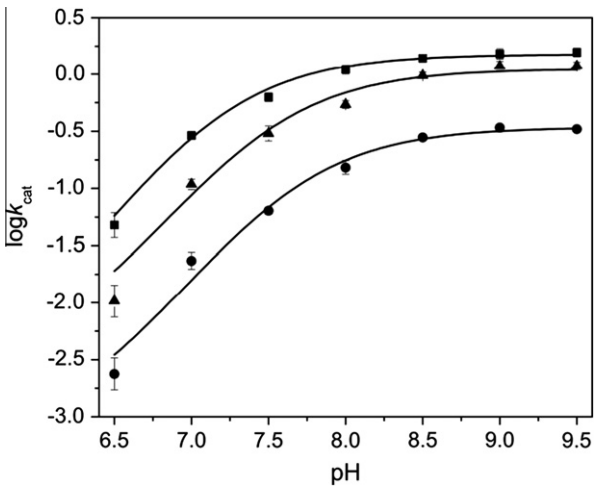

Fig. 3. pH dependence profile for turnover of wild type (closed rectangles) and the H225Q (triangles) and H225A (circles) mutants of OAM. Data were fit to Eq. (2) and k_{cat} was measured as described in Materials and methods.

substrate to PLP and an increase in absorbance at 358 nm, representing formation of cob(III)alamin at the rate of ~0.06 min^{-1} (Fig. 4A and C). The fact that the rate of cob(III)alamin formation is similar between the OAM variants indicates that the His225 mutants do not succumb to enzyme inactivation more than the native enzyme. It is interesting to note that upon addition of D-ornithine to H225A, the absorbance change at 525 nm (Fig. 4C) is negligible, indicating that homolysis of AdoCbl is catalytically restricted in this mutant.

The binding of the inhibitor, DABA, to wild type and the H225A and H225Q mutants leads to formation of an external aldimine (absorbance decrease at 410; Figs. S2B, 4C and 4D). However, in contrast to the natural substrate, binding of DABA leads to an absorbance peak at 470 nm in native OAM, representing cob(II)alamin formation (Fig. S2B). Previous EPR data show that the paramagnetic Co^{2+} metal center of the cob(II)alamin cofactor is tightly coupled to the 2,4-diaminobutyryl-PLP organic radical [11]. With wild type OAM, there is no discernable formation of cob(III)alamin during the 30 min time course of the reaction, emphasizing the stable nature of the 2,4-diaminobutyryl-PLP radical intermediate (Fig. S2B). UV-absorbance changes following the addition of DABA to the H225Q and H225A mutants are distinctive from wild type. As for the native enzyme, binding of the inhibitor leads to a decrease at 416 nm indicating formation of an external aldimine. There is also a peak at 470 nm (reflecting formation of cob(II)alamin), but in both mutants there is a relatively rapid increase in absorbance at 358 nm, suggesting that the biradical state of the enzyme is unstable as cob(II)alamin loses an electron to form cob(III)alamin by a pathway that is independent of O_2. Comparison of the UV-absorbance spectra between the two His225 mutants in Fig. 4C and D reveals that there is less AdoCbl homolysis (absorbance change at 525 nm) and cob(II)alamin (absorbance peak at 416 nm) in H225A compared to H225Q. The rate of cob(III)alamin formation is also slower in H225A (0.10 min^{-1}) compared to H225Q (0.23 min^{-1}), supporting the observation that there is less overall radical formation for this mutant. Less efficient AdoCbl homolysis may also account for slower steady state turnover by the OAM H225A variant.

3.5. Aerobic UV-visible spectroscopic assays

To determine if the His225 mutants make the enzyme more susceptible to O_2 inactivation (causing oxidation of cob(II)alamin to cob(III)alamin), the UV visible absorbance assays were repeated under aerobic conditions (Fig. 5). During turnover with D-ornithine, the rate constant for cob(III)alamin formation (measured as an absorbance increase at 358 nm) is 0.4 min^{-1} for wild type OAM. This rate increases ~4 fold in the OAM–DABA complex, likely due to the prolonged presence of cob(II)alamin in the active site and therefore increased susceptibility to O_2. Mutation of His225 to glutamine or alanine decreases the sensitivity of the enzyme to O_2 inactivation with D-ornithine and DABA. The rate constants for cob(III)alamin formation with H225A and H225Q mutants with D-ornithine are 0.13 and 0.07 min^{-1}, respectively, while the corresponding rate constants for the two mutants with DABA are 0.15 and 0.33 min^{-1} (Fig. 4B). The reduced sensitivity of the mutant enzymes to O_2 suggests less cob(II)alamin in the active site upon binding of the substrate or inhibitor. This may arise from less efficient AdoCbl Co–C bond homolysis leading to slower cob(II)alamin formation, as has been suggested from anaerobic UV-visible spectral assays involving H225A. Alternatively, competing side reactions may also reduce the level of cob(II)alamin in the active site.

3.6. Spectroscopic properties of the PLP-bound OAM

UV-visible spectroscopy was also used to determine if the His225 mutants perturb the protonation state of the Schiff base

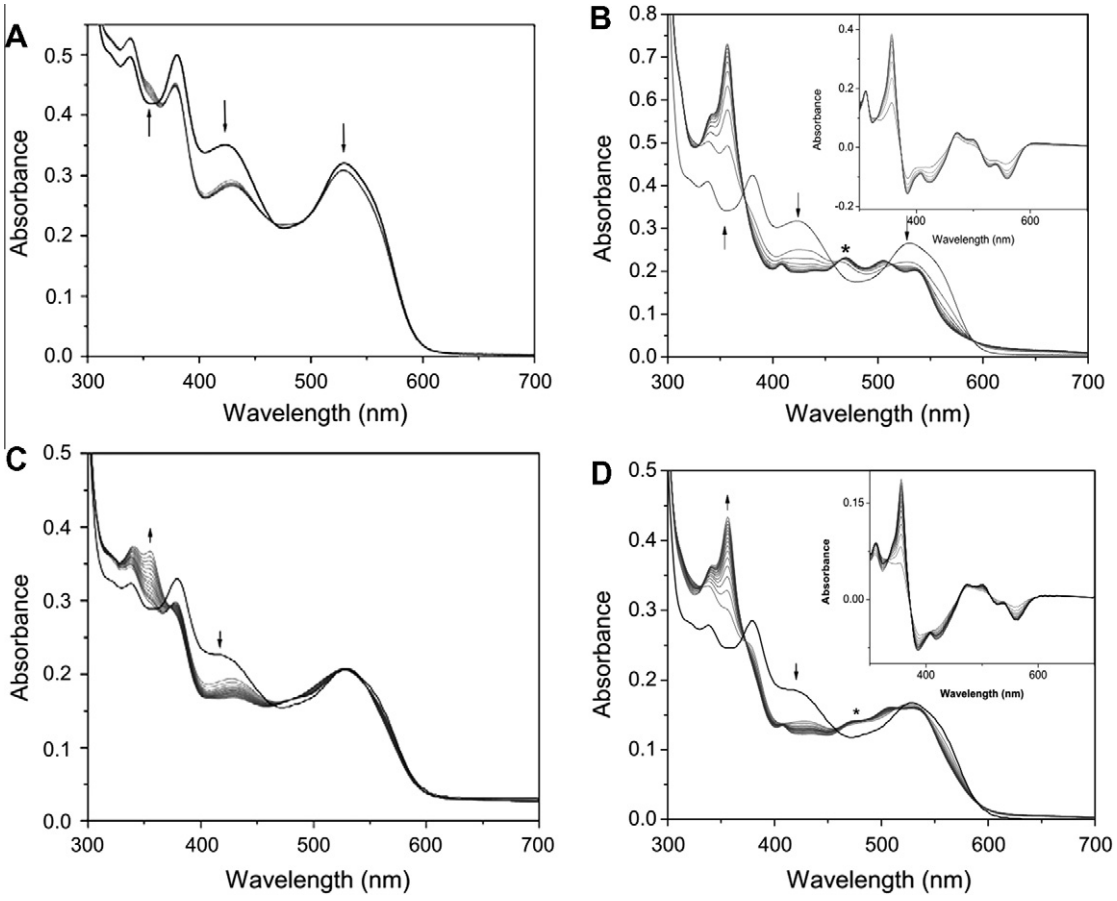

Fig. 4. Anaerobic UV-visible spectral changes of holo-OAM H225Q and H225A mutants following the addition of D-ornithine and 2,4-diaminobutyric acid. The holoenzyme solution contains 100 mM NH_4^+EPPS, pH 8.5, 15 μM OAM, 15 μM PLP and 15 μM AdoCbl. Spectral changes in H225Q (A and B) and H225A (C and D) holo-OAM were recorded before (black line) and after (grey lines) the addition of 2.5 mM D-ornithine (A and C) and 2, 4 diaminobutyric acid (B and D). Spectra were recorded every 2 mins for 30 mins.

of the external aldimine with either D-ornithine or DABA bound to the enzyme. Scheme 1 illustrates the two PLP tautomers of the external aldimine that arise from internal proton transfer from the imino nitrogen and the 3-oxo anion of the pyridine ring. A hydrogen bonded iminium zwitterion (A) forms upon protonation of the Schiff base; this tautomer has an absorption maximum between 401 and 415 nm. Internal proton transfer to the phenolic oxygen generates a hydrogen-bonded imine (B1), with an absorption maximum between 325 and 330 nm. If His225 acts as a hydrogen bond acceptor to the phenolic oxygen, it may shift the equilibrium towards the hydrogen-bonded imine state of the cofactor, by favoring the B2 intermediate of Scheme 1. To observe a change in the equilibrium distribution of the PLP tautomers, absorbance spectra were recorded for OAM with only PLP bound to the enzyme (referred to as PLP–OAM), as the absorbance spectrum of AdoCbl partially masks that of PLP. Fig. 6A shows that the D-ornithinyl–PLP external aldimine (at pH 8.5) is a mixture of the hydrogen bonded imine (absorbance shoulder at 330 nm) and hydrogen bonded iminium zwitterion (absorbance peak at 415 nm) with the major species being the latter form (Fig. 6A). This indicates that the N^{δ} aldimine is predominantly protonated in the D-ornithinyl–PLP–OAM complex (without AdoCbl). In contrast, loading of DABA onto PLP–OAM results in a shift of the tautomeric distribution towards the hydrogen bonded imine (Fig. 6B). The UV-visible spectra of the D-ornithinyl–PLP and 2,4-diaminobutyryl–PLP aldimines in both of the His225 mutants are similar to wild type in that the predominant species is the iminium zwitterion (Fig. 6A) with the natural substrate, whereas the binding of DABA shifts the equilibrium towards the imine state (B in Scheme 1). These data suggest that direct hydrogen bonding between the imidazole of His225 and the phenolic group does not significantly influence the protonation state of the Schiff base upon non-enzymatic condensation of the cofactor with the substrate or inhibitor in PLP–OAM. However, there still remains the possibility that His225 influences the pK_a of the Schiff base in the holoenzyme at different steps of the catalytic cycle.

4. Discussion

PLP-dependent enzymes catalyze a diverse array of biological transformations of amino acids and other amine-containing substrates, including transaminations, racemizations, decarboxylations, and β- and γ-eliminations and replacements. For each of these reactions, PLP facilitates catalysis by stabilizing an α-carbanion catalytic intermediate by electronic delocalization through the conjugated π system of the pyridine ring and Schiff base. Computational and experimental work has highlighted the importance of ionizable groups of the cofactor (i.e. phenolic oxygen, imino nitrogen, and pyrimidine nitrogen) in mediating resonance stabilization of polar intermediates [15,18]. Moreover, external hydrogen bond donors and acceptors to the PLP phenolic oxygen and pyridine nitrogen have been shown to finely tune the catalytic role of the PLP cofactor [19,20]. However, little is known how corresponding residues in PLP-dependent aminomutases participate in catalysis. For this group of enzymes, which includes lysine 2,3-aminomutase, arginine 2,3-aminomutase and glutamate 2,3-aminomutase, PLP assumes an unusual role in catalysis: the

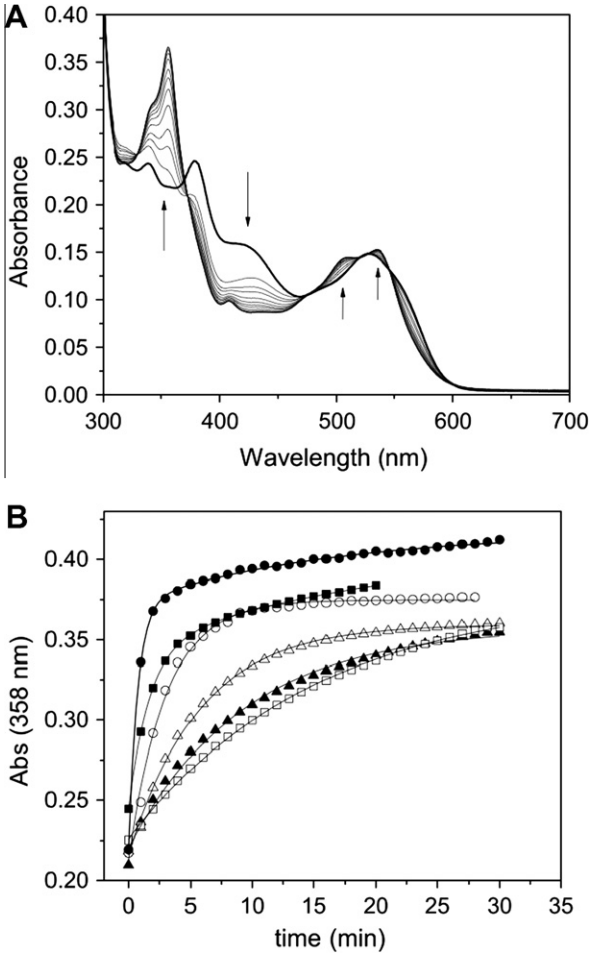

Fig. 5. Aerobic formation of cob(III)alamin by wild type OAM and H225A and H225Q mutants in the presence of D-ornithine and 2,4-diaminobutyric acid. Panel A, UV visible absorption spectra of holoOAM H225A mutant before (blank line) and following addition of addition of DABA (grey lines). The solution contained 15 μM OAM, 15 μM PLP, and 15 μM AdoCbl in 100 mM NH_4^+EPPS in a total volume of 995 μL. The reaction was started by the addition of 5 μL of 2.5 mM inhibitor. Spectra were recorded every minute for 30 minutes at 20 °C. Only representative spectra are shown. (B) The rate of cob(III)alamin formation was followed for wild type holo-OAM with D-ornithine (filled squares) and 2,4-diaminobutyric acid (filled circles), OAM H225Q with D-ornithine (open squares) and 2,4-dimaminobutyric acid (open circles), and H225A with D-ornithine (filled triangles) and with 2,4-diaminobutyric acid (open triangles). Data were fit to a single exponential equation to determine the observed rates for cob(III)alamin formation.

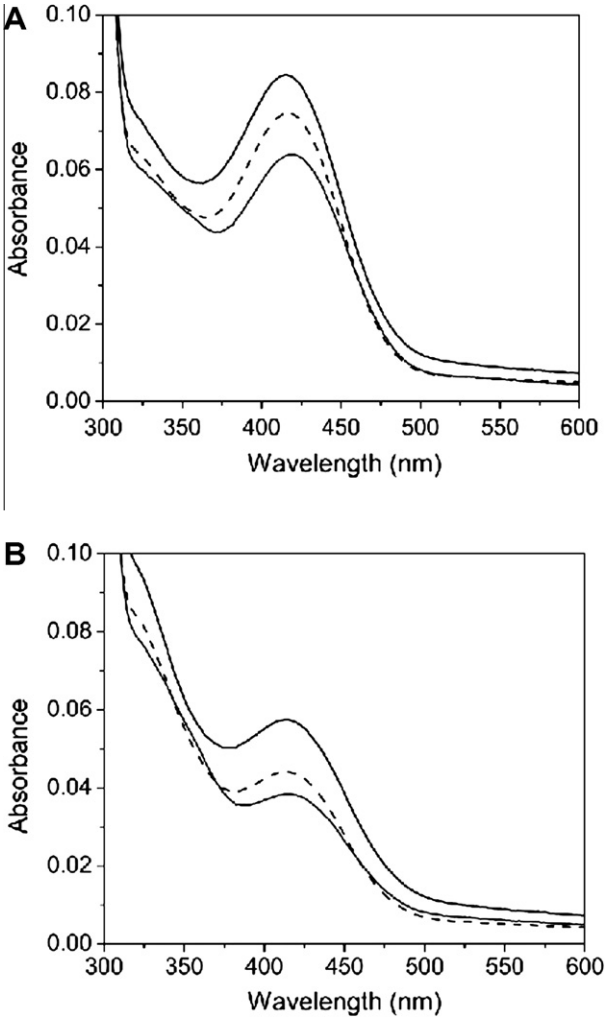

Fig. 6. Distribution of tautomers of (A) D-ornithyl–PLP external aldimine and (B) 2,4 diaminobutyryl–PLP external aldimine (B) in wild type (black), H225Q (dashed) and H255A (grey). An equimolar mixture of apo-OAM (15 μM) and PLP (15 μM) was mixed in a total volume of 995 μl in 100 mM NH_4^+EPPS, pH 8.5, at 25 °C in an anaerobic environment. Following a 5 min incubation, 2.5 mM D-ornithine (Panel A) or 2.5 mM DL-2,4-diaminobutyric acid (Panel B) was added to the reaction mixture in a 5 μl volume. Following a further 5 min incubation the spectra were recorded from 300 to 600 nm.

stabilization and isomerization of nonpolar radical intermediates. Here in this study, we chose to investigate the role of His225 as it is within hydrogen bond contact to the phenolic oxygen of PLP, and therefore in a position to participate in catalysis by influencing the protonation state of the imino nitrogen.

The steady state kinetic experiments show that His225 participates in catalysis. The fact that the H225A mutant results in a larger reduction in turnover compared to the H225Q mutant suggests that a glutamine side chain can partially substitute for the histidine imidazole moiety, perhaps through formation of a hydrogen bond to the PLP phenolic oxygen or by maintaining a modestly bulky side chain in the active site. The pH studies show that the rate of catalysis is dependent on the deprotonation of an ionizable group, but the residue is not His225 as each of the three forms of OAM tested show similar pH profiles and pK_a values. The ionizable group may be the internal or external aldimine, known to have pK_a values within this range [21]. If this were the case, then it suggests that aldiminium ionization limits catalysis. Alternatively, the ionizable group may be another active site residue on OAM or DAPDH.

It is interesting to note that structurally-related 5,6-LAM, which performs 1,2-amino shifts on both D-lysine and β-L-lysine, undergoes suicide inactivation (involving direct electron transfer from cob(II)alamin to a PLP-substrate/product radical intermediate) at a rate that is 10-fold higher than OAM [22]. An overlay of the PLP binding sites in OAM and 5,6-LAM reveals that the majority of residues that interact with PLP are conserved between OAM and 5,6-LAM; the exception is His225 in OAM. Asp289 in 5,6-LAM most closely overlays with His225, but does not form a polar interaction with the cofactor [9]. Our data suggest that this minor structural difference does not account for apparent differences in the ability of the enzyme to stabilize and control the trajectories of radical intermediates during catalysis. It remains unclear why suicide inactivation is a more prominent feature of 5,6-LAM catalysis compared to OAM, but it may involve other structural features that fine-tune the stability of PLP–radical intermediates or control the timing of AdoCbl homolysis.

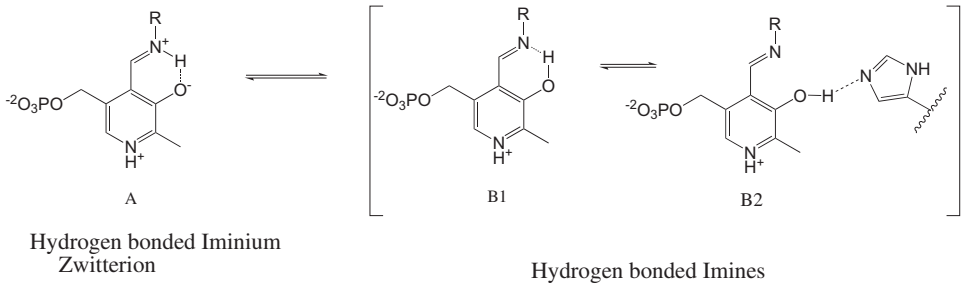

Scheme 1.

In the presence of O_2, the rate of cob(III)alamin formation is much greater in the presence of DABA compared to D-ornithine due to the lingering presence of the metallo-paramagnetic species in the active site. The susceptibility of the enzyme to O_2 in the presence of D-ornithine or DABA is diminished in H225Q and to a greater extent in the H225A mutant, presumably because of the shortened lifetime of cob(II)alamin in the active site. With the H225A mutant, AdoCbl homolysis is noticeably reduced (not detectable by UV-visible spectroscopy), which likely explains impeded catalytic turnover and attenuated side reactions with O_2. A decrease in AdoCbl bond homolysis in the H225A mutant may be linked to improper positioning of the C4 carbon of the ornithinyl-PLP side chain for hydrogen abstraction by the 5′-deoxyadenosyl radical. Previous studies with related AdoCbl-dependent enzymes have shown that these two kinetic steps, Co–C bond homolysis and hydrogen abstraction from the substrate, are tightly coupled [23]. Alternatively, AdoCbl homolysis may also be tightly coupled to steps further along the catalytic cycle, i.e. formation of the aziridinylcarbinyl–PLP radical. If the energy barriers were elevated for these downstream catalytic steps, one would also expect attenuation of Co–C homolytic rupture.

For the H225Q mutant, UV-visible spectroscopy clearly shows that AdoCbl homolysis occurs as for wild type. However, the cob(II)alamin that does form upon loading of the enzyme with DABA collapses to form cob(III)alamin by a mechanism that is independent of O_2. This is also observed with H225A, albeit to a lesser degree. To rationalize why cob(II)alamin, which is presumably coupled to the 2,4-diaminobutyryl–PLP derived radical, is less stable in the H225 mutants compared to wild-type, the crystal structures of OAM with DABA and D-ornithine were closely investigated (Fig. 2). D-ornithine is secured to the active site through electrostatic/polar interactions between the α-carboxylate and the side chain Arg297 and between the α-amine and carboxylate of Glu81. As a result of these interactions, the D-ornithinyl–PLP aldimine is positioned such that the p-orbitals of the Schiff base and pyridine nitrogen are aligned for optimal electronic delocalization of ensuing radical intermediates. The crystal structure of OAM-DABA complex also shows that the α-carboxylate of the inhibitor forms a salt bridge with Arg297, despite having one less carbon atom in the side chain. As a consequence, the p-orbitals of the Schiff base of the external aldimine are not optimally aligned with the pyridine ring. This would then suggest that upon abstraction of the C4 hydrogen atom by the 5′-deoxyadenosyl radical from 2,4-diaminobutyryl–PLP aldimine, the radical localized to the C4 atom is principally stabilized though resonance stabilization involving the imine and not the conjugated π-system of the pyridine ring. If this were the case, then a deprotonated imino nitrogen likely leads to greater resonance stabilization of the C4 radical. For wild type OAM, His225 may be acting as a general base to the phenolic oxygen, which would favor the deprotonated state of the imino nitrogen (B2 in Scheme 1). Mutation of His225 would likely shift the position of the bridging proton towards the imino nitrogen, causing it to be more sp^3-like, leading to collapse of the organic radical. Steady state inhibition studies reveal that His225 contributes to the binding of 2,4-diaminobutyric acid. Although, the X-ray crystal structure of the OAM-DABA complex does not reveal direct hydrogen bonding between the His225 imidazole side chain and the PLP-bound inhibitor, the two moieties are within van der Waals contact, and this weak noncovalent interaction may partially contribute to the inhibitor binding affinity.

From UV-visible spectral studies, it is evident that the D-ornithinyl–PLP aldimine is predominantly in the hydrogen bonded iminium zwitterion state without AdoCbl bound to the enzyme. A number of factors contribute to the tautomeric equilibrium of the Schiff base, such as the substituent on the imino group and the localized polar environment [24,25]. Upon formation of the catalytically closed complex in the holoenzyme, a prerequisite for PLP-mediated radical rearrangement, the solvent polarity around the PLP external aldimine is expected to change, and this likely shifts the position of the bridging proton between the phenolic oxygen and the imino nitrogen. Thus, it is not clear which prototropic tautomer, if any, predominates at the start of the catalytic cycle. Following abstraction of the C4 hydrogen atom from the substrate, the next step in the proposed catalytic cycle involves formation of the aziridinylcarbinyl–PLP radical. This cyclic intermediate arises from reversible radical addition involving unpairing of the π electrons of the imine group. Deprotonation of the imino nitrogen, possibly facilitated by proton abstraction from His225, lowers the energy barrier for ring closure. Computational calculations by Wetmore et al. revealed that the N—H—O intramolecular bridge of PLP was integral in preventing overstabilization of the cyclic radical intermediate by disrupting optimal alignment of p-orbitals and minimizing captodative stabilization of the radical intermediate [14]. Thus, ring opening may involve partial proton transfer back to the phenolic oxygen, again possibly facilitated by His225, to avoid deep energy wells along the reaction coordinate, a key goal of catalysis. Thus, His225 may finely tune radical rearrangement by participating in partial proton transfer with PLP, thereby lowering the energy barrier for ring closure and opening. *Ab initio* calculations have previously alluded to the importance of protonation or partial protonation of the migrating group being critical for facilitating 1,2 shifts in other AdoCbl-dependent enzymes [26–29].

In conclusion, our data indicate that His225 plays a role in catalysis; *via* its interaction with the phenolic oxygen, the imidazole side chain may serve as a site for partial proton transfer during catalysis, enabling efficient intramolecular cyclization. Mutation of the residue does not increase the enzyme's susceptibility to uncontrolled catalysis during turnover with D-ornithine, suggesting that trajectories and stability of radical intermediates are preserved. His225 does however contribute to the overstabilization of the 2,4-diaminobutyryl–PLP radical species by acting as a general base to the phenolic oxygen, lowering the pK_a of the imino

nitrogen which in turn favors resonance delocalization of the unpaired electron through the Schiff base. We are currently testing this model through computational calculations.

Acknowledgments

This work is supported by a grant from the Natural Sciences and Engineering Research Council of Canada and the UK Biotechnology and Biological Sciences Research Council (BBSRC). NSS is a BBSRC Professorial Research Fellow and a Royal Society Wolfson Merit Award holder.

Appendix A. Supplementary material

Supplementary data associated with this article can be found, in the online version, at doi:10.1016/j.bioorg.2011.08.003.

References

[1] J.K. Dyer, R.N. Costilow, Journal of Bacteriology 96 (1968) 1617–1622.
[2] T.C. Stadtman, F.H. White Jr., Journal of Bacteriology 67 (1954) 651–657.
[3] T.D. Lawley, N.J. Croucher, L. Yu, S. Clare, M. Sebaihia, D. Goulding, D.J. Pickard, J. Parkhill, J. Choudhary, G. Dougan, Journal of Bacteriology 191 (2009) 5377–5386.
[4] N. Fonknechten, A. Perret, N. Perchat, S. Tricot, C. Lechaplais, D. Vallenet, C. Vergne, A. Zaparucha, D. Le Paslier, J. Weissenbach, M. Salanoubat, Journal of Bacteriology 191 (2009) 3162–3167.
[5] N. Fonknechten, S. Chaussonnerie, S. Tricot, A. Lajus, J.R. Andreesen, N. Perchat, E. Pelletier, M. Gouyvenoux, V. Barbe, M. Salanoubat, D. Le Paslier, J. Weissenbach, G.N. Cohen, A. Kreimeyer, BMC Genomics 11 (2010).
[6] H.P. Chen, F.C. Hsui, L.Y. Lin, C.T. Ren, S.H. Wu, European Journal of Biochemistry 271 (2004) 4293–4297.
[7] M.D. Ballinger, P.A. Frey, G.H. Reed, Biochemistry 31 (1992) 10782–10789.
[8] K.R. Wolthers, C. Levy, N.S. Scrutton, D. Leys, Journal of Biological Chemistry 285 (2010) 13942–13950.
[9] F. Berkovitch, E. Behshad, K.H. Tang, E.A. Enns, P.A. Frey, C.L. Drennan, Proceedings of the National Academy of Sciences of the United States of America 101 (2004) 15870–15875.
[10] K.H. Tang, S.O. Mansoorabadi, G.H. Reed, P.A. Frey, Biochemistry (2009).
[11] K.R. Wolthers, S.E. Rigby, N.S. Scrutton, Journal of Biological Chemistry 283 (2008) 34615–34625.
[12] R. Reitzer, K. Gruber, G. Jogl, U.G. Wagner, H. Bothe, W. Buckel, C. Kratky, Structure 7 (1999) 891–902.
[13] N. Shibata, H. Tamagaki, N. Hieda, K. Akita, H. Komori, Y. Shomura, S. Terawaki, K. Mori, N. Yasuoka, Y. Higuchi, T. Toraya, Journal of Biological Chemistry 285 (2010) 26484–26493.
[14] S.D. Wetmore, D.M. Smith, L. Radom, Journal of the American Chemical Society 123 (2001) 8678–8689.
[15] M.D. Toney, Archives of Biochemistry and Biophysics 433 (2005) 279–287.
[16] R. Somack, R.N. Costilow, Biochemistry 12 (1973) 2597–2604.
[17] H.P. Chen, S.H. Wu, Y.L. Lin, C.M. Chen, S.S. Tsay, Journal of Biological Chemistry 276 (2001) 44744–44750.
[18] R. Casasnovas, A. Salva, J. Frau, J. Donoso, F. Munoz, Chemical Physics 355 (2009) 149–156.
[19] Y.L. Lin, J.L. Gao, Biochemistry 49 (2010) 84–94.
[20] Y. Shiraiwa, H. Ikushiro, H. Hayashi, Journal of Biological Chemistry 284 (2009) 15487–15495.
[21] H.H. Limbach, M. Chan-Huot, S. Sharif, P.M. Tolstoy, M.D. Toney, Biochemistry 49 (2010) 10818–10830.
[22] K.H. Tang, C.H. Chang, P.A. Frey, Biochemistry 40 (2001) 5190–5199.
[23] R. Padmakumar, R. Banerjee, Biochemistry 36 (1997) 3713–3718.
[24] S. Sharif, D. Schagen, M.D. Toney, H.H. Limbach, Journal of the American Chemical Society 129 (2007) 4440–4455.
[25] S. Sharif, G.S. Denisov, M.D. Toney, H.H. Limbach, Journal of the American Chemical Society 129 (2007) 6313–6327.
[26] S.D. Wetmore, D.M. Smith, B.T. Golding, L. Radom, Journal of the American Chemical Society 123 (2001) 7963–7972.
[27] D.M. Smith, B.T. Golding, L. Radom, Journal of the American Chemical Society 123 (2001) 1664–1675.
[28] D.M. Smith, B.T. Golding, L. Radom, Journal of the American Chemical Society 121 (1999) 9388–9399.
[29] D.M. Smith, B.T. Golding, L. Radom, Journal of the American Chemical Society 121 (1999) 1383–1384.